Effect of postural alignment alteration with age on vertebral strength

Cécile Heidsieck (1), Laurent Gajny (1), Christophe Travert (2), Jean-Yves Lazennec (2), Wafa Skalli (1)

1. Arts et Métiers ParisTech, Institut de Biomécanique Humaine Georges Charpak, Paris, France

2. Department of Orthopaedic and Trauma Surgery, Pitié-Salpétrière Hospital, Assistance Publique-Hopitaux de Paris, Sorbonne University, Paris France.

Corresponding author: Cécile Heidsieck, cecile.heidsieck@ensam.eu, ORCID : 0000 0001 8331 0669

Mini Abstract. EOS biplane radiographs of 117 subjects between 20 and 83 years were analyzed to compute the upper body lever arm over the L1 vertebra and its impact on vertebral strength. Postural sagittal alignment alteration was observed with age and resulted in a greater lever arm causing vertebral strength to decrease.

Purpose. The purpose of this study was to analyze the impact of postural alignment changes with age on vertebral strength using finite element analysis and barycentremetry.

Methods. A total of 117 subjects from 20 to 83 years were divided in three age groups: young, (20 to 40 years, 62 subjects), intermediate (40 to 60 years, 26 subjects) and elderly (60 years and over, 29 subjects). EOS biplane radiographs were acquired, allowing 3D reconstruction of the spine and body envelope as well as spinal, pelvic and sagittal alignment parameters measurements. A barycentremetry method allowed estimating of the mass and center of mass (CoM) position of the upper body above L1, relatively to the center of the L1 vertebra (lever arm). To investigate the effect of this lever arm, vertebral strength of a generic finite element models (with constant geometry and mechanical properties for all subjects) was successively computed applying the personalized lever arm of each subject.

Results. A combination of an increase in thoracic kyphosis, cervical lordosis and pelvic tilt with a loss of lumbar lordosis was observed between the young and the older groups. Sagittal alignment parameters indicated a more forward position as age increased. The lever arm of the CoM above L1 varied from an average of 1 mm backward for the young group, to averages of 7 and 24 mm forward, respectively for the intermediate and elderly group. As a result, vertebral strength decreased from 2527 N for the young group to 1820 N for the elderly group.

Conclusion. The global sagittal alignment modifications observed with age were consistent with the literature. Posture alteration with age reduced vertebral strength significantly in this simplified loading model. Postural alignment seems essential to be considered in the evaluation of osteoporotic patients.

Keywords : vertebral strength, finite element method, barycentremetry, global sagittal alignment, osteoporosis

Declarations

Acknowledgments

Introduction

Vertebral fragility fractures associated with osteoporosis are a major health problem, because they increase morbidity and mortality [1, 2]. A precise fracture risk estimation is a key factor to limit the negative consequences of those fractures and offer the appropriate treatment to the population at risk. Areal bone mineral density (aBMD) measurement with dual-energy X-ray absorptiometry (DXA) is the reference technique to evaluate fracture risk, but its sensitivity is low [3, 4]. The conditions leading to vertebral fractures are complex and still to be explored. Depending on the studies, the causes of 27% to 38% fragility fractures are not identified [5, 6]. Other parameters than the aBMD can be taken into account to improve the fracture risk estimation. Recent studies showed that sagittal alignment could have an impact on vertebral fracture occurrence. Hu et al [7] showed a negative correlation between an alteration of the sagittal alignment and the quality of life. Also, an abnormal forward spinal inclination was found in subjects consulting for osteoporosis, even for those without vertebral fractures [8]. This inclination increases with age [9, 10], translating a tendency to have a more forward position in the elderly population.

Finite element models (FEM) based on quantitative computer tomography (qCT) were developed to allow vertebral strength estimation with personalized mechanical properties and geometry. In brief, these models use the personalized geometry of a vertebra reconstructed from the CT-scan. The vertebra is then split into small elements, typically around 1 millimeter wide. Then each element is given specific mechanical laws depending on the volumetric BMD (vBMD) measured in this specific location in the vertebra. Then a compression force is simulated on the vertebral body to estimate its mechanical behavior and more specifically its strength. verterbral qCT-based FEM were validated with experimental data [11–13]. They are now used in clinical studies to evaluate strength changes following osteoporosis treatments [14]. Vertebral fracture incidence prediction accuracy through qCT based FEM was recently assessed. It was compared to aBMD and volumetric BMD measurements. The strength obtained through qCT based FEM showed to be more correlated to vertebral fracture incidence than aBMD values but equivalent to vBMD measurements [15]. Parameters taken into account by qCT based FEM might not be enough to fully predict fragility fractures. Indeed, the occurrence of a fracture depends as much on the strength of the bone as on the load that is applied to it. Subject-specific loading conditions could provide complementary information.

Musculoskeletal models have been used to estimate spinal loads in subjects with spinal deformities. Briggs et al [16] indicated that subjects with hyperkyphosis could experience compressive loads 14% greater than subjects with lower kyphosis in a relaxed position. Compensatory mechanisms to prevent the gravity line from shifting forward can limit the phenomenon [17]. However, studies have shown that loading conditions on the spine were critical [18, 19]. A sensitivity study on loading conditions on finite element modelled vertebrae revealed that displacing the load application anteriorly by 1cm resulted in a decrease up to 60% of the vertebral strength [19].

In the upright position, loads on the vertebrae result from the balance between gravity loads due to the upper body weight and the forces of muscles surrounding the spine. The gravity loads supported by the intervertebral disks and the vertebral bodies depend on the mass and center of mass of the upper body segments, which results from the upper body shape and alignment [20]. Barycentremetry is a method to estimate the mass and center of mass of each body segment [20]. It uses a combination of the three-dimensional body geometry reconstruction and body segment density estimation. Recent models have allowed the computation of the whole body mass as well as the center of mass (CoM) position based on barycentremetry methods from biplanar X-Rays. First, the simultaneous acquisition of frontal and sagittal head to feet X-rays allows 3D reconstruction of the spine [21, 22] and body envelope [23] in the standing position. Then, density models for each body segment are used to estimate the mass and CoM of the body parts above a given vertebra [24].

No study has yet combined FEM with barycentremetry to evaluate posture and morphology effect on potential vertebral fracture occurrence. The aim of this study is to investigate the impact of the aging process on sagittal alignment and on the forces applied on a vertebra, and therefore on its risk of fracture. We assume that morphological and postural modifications with age can be quantified and should be considered in the vertebral fracture risk prediction.

Materials and methods

Population inclusion criteria:

Retrospective clinical data from previous studies were used. Subjects included were asymptomatic volunteers who had low dose bi-planar X-ray radiographs after approval by the Ethics Committee [Comité de Protection des

Personnes CPP No 2010/113 and CPP No 06036]. The bi-planar X-ray images were obtained with the EOS system (EOS imaging, Paris, France) [25], a low dose system which can obtain simultaneously two head to feet radiographs in the frontal and the sagittal plan with two X-ray sources. Subjects had to stand in the standardized freestanding position [26] with hand resting either on the mandibles or on the clavicles and had to look horizontally.

Clinical exams were performed to ensure that the subjects presented no symptomatic lower limb nor spine pathology that could affect the spinal alignment and patient with a frontal cobb angle more than 20° were excluded. In total, 117 subjects (59 males, 58 females, all Europeans) were included. The mean age was 43 (1SD = 19, min = 20, max=83). We divided the volunteers in three age groups: 62 young (32 males, 30 females, mean age = 27 , 1SD =5, min = 20, max = 39), 26 intermediate (1 males, 12 females, mean age = 49, 1SD 6, min = 40, max = 59), and 29 elderly (13 males, 16 females, mean age = 70, 1SD = 5, min = 62, max = 83) subjects. The body mass index (BMI) was computed for the subjects of which the height and weight were available (90/117).

3D reconstruction:
The radiographs were processed to perform 3D reconstructions of the spine [22, 27], pelvis [21], odontoid process (OD) location and external body envelope [23], using validated methods.

Radiographic parameters:
Several parameters were measured on the 3D reconstruction to describe the sagittal spine alignment. 1/ Spinal curvatures: C3-C7 cervical curvature, T4-T12 thoracic kyphosis and L1-S1 lumbar lordosis. 2/ Pelvic parameters: pelvic incidence (PI), sacral slope (SS) and pelvic tilt (PT) [28]. 3/ Three global sagittal alignment parameters (figure 1): SVA, OD-HA sagittal angle and spinal inclination [OD-S1]. The.SVA (sagittal vertical axis) was defined as the sagittal distance between the center of C7 vertebral body and the posterior corner of the sacral superior endplate (figure 1a) [29]. The.OD-HA (middle of the centers of each acetabulum) angle was defined as the sagittal angle between the vertical and the line across OD-HA (figure 1b) [30]. The spinal inclination [OD-S1], was defined as the angle between the vertical and the line of best fit across the following points: OD, all vertebral centroids between C3 and L5 and the center of the sacral superior endplate (figure 1c) [31]

Barycentremetry:
Estimation of the center of mass (CoM) above the vertebral level L1 was performed for each subject using barycentremetry from the EOS images, as described by Amabile et al [32]. The method is briefly reminded hereafter. The external body envelope was reconstructed using EOS images. Although the images were acquired with hands resting on the clavicle or on the mandibles, upper limbs were virtually placed in a neutral position along the body in the model to locate the CoM (figure 2a). Then, the body envelope was divided in body segments of which the volume and mass was computed using an improved Dempster Uniform density method [32]. The CoM of each body segment was then computed and used to compute the CoM of the whole body above the superior endplate of L1.

The thoraco-lumbar junction, including the L1 level, is where most of the of vertebral fractures in osteoporotic subjects occurs [33, 34]. Therefore, we focused the study on the L1 vertebral level.

This CoM is not necessarily vertically aligned with the L1 vertebra. The distance between the vertical line going through the CoM and the L1 vertebra creates a torque that adds up to the load on the vertebra, which is proportional to this distance times the magnitude of the force. This distance is called lever arm (or moment arm).It was defined as the horizontal distance between the upper body CoM and the center of the superior endplate of L1. It was measured in the lateral and anteroposterior directions. As the 3D orientation of the vertebra affects the ability of the vertebra to resist to applied strength, it also was reported in the axial, frontal and sagittal plane.

Finite element analysis:
To study the impact of the lever arm of the CoM, and the 3D orientation of the vertebra, a previously validated vertebral FEM was used [13]. In the current study, since no data was acquired to study bone mineral density on the subjects, we used three different models extracted from this previous study. To choose these models, three classes of vertebrae (weak, normal and strong) were made depending on their strength in anterior compression, and one vertebral model was chosen close to the center of each class. The weak vertebra had a vBMD of 86 mg/cm3 and a strength of 1935 N, the normal vertebra had a vBMD of 86 mg/cm3 and a strength of 3229 N, and the strong vertebra had a vBMD of 190 mg/cm3 and a strength of 5091 N. The corresponding vBMD and elastic modulus of the three strength models are the following, weak: 71 mg/cm3, 192 MPa; normal: 86 mg/cm3, 240 MPa; strong: 190 mg/cm3, 576 MPa. Those three vertebral models had their own geometry and material properties

These three models were used to perform simulation for all subjects of the study. We personalized only the boundary conditions to match the 3D orientation of the subject's L1 vertebra, and the lever arm of the upper body CoM.

The finite element model is detailed in [13] and briefly described hereafter. Geometry of the vertebrae used for the model was obtained by a semi-automatic segmentation method [35] and a hexahedral mesh of the vertebrae was generated. Mechanical properties were linear elastic and were set for each element depending on the bone density measured in the corresponding voxels of the qCT-scan.

Thin layers of polymethyl methacrylate (PMMA) bone cement were virtually added on the upper and lower vertebral endplates for parallelism to ensure uniform loading conditions. The orientation of the vertebral model was adjusted to match the orientation of the subject's L1 vertebra. Lower nodes of the PMMA layer were constrained in all degree of freedom. A compressive load was applied to a node located at the position of the upper body center of mass of each subject and was joined by rigid elements to the upper PMMA layer (figure 2b).

The simulations were run on ANSYS software (ANSYS Inc, Canonsburg, PA, USA). The failure criteria chosen to describe vertebral strength was set when a contiguous region of 1 mm^3 of elements reached 1.5% deformation [35].

Load to strength ratio:
To integrate the body mass variations, a load to strength ratio was also computed. The load resulted in the upper body mass above L1 as estimated by the barycentremetric model and the strength was the one computed using the personalized lever arm. Theoretically, when the ratio is higher than 1, the load exceeds bone strength and a fracture will occur.

Data analysis:
Normality of the data was assessed with the Shapiro-Wilk normality test. Differences between groups were evaluated with Student tests (in case of normality) and Wilcoxon rank-sum tests (otherwise).

Results

Clinical parameters and differences between groups:
All the studied parameters followed a normal distribution, except for age. The results are presented in the table 1 with mean (M) and standard deviation (SD).

The BMI tended to increase with age and was significantly higher in the older group compared to the younger group.

Regarding pelvic parameters, no significant changes in pelvic incidence with age were observed. Pelvic tilt increased significantly from 9.4 to 18° and sacral slope decreased significantly from 41.1 to 36.1° between the young and the elderly groups.

Concerning spinal parameters, a significant loss of lumbar lordosis as well as a significant increase in the thoracic kyphosis and in the cervical curvature lordosis (indicated by the transition from a positive to a negative value) were observed between the young and the older groups.

The sagittal alignment parameters (OD-HA sagittal angle, SVA, spinal inclination [OD-S1]) all showed a narrow range of variation between all age groups, but with a tendency to increase as age is higher. Significant differences between the young group and the elderly group were observed for the three parameters. However, significant differences between the young group and the intermediate group were only observed for the SVA and the spinal inclination [OD – S1].

L1 orientation and upper body CoM's lever arm regarding L1:
The axial and frontal orientation of L1 was not significantly different between the age groups, and close to zero degree. On the other hand, the sagittal orientation of L1 varied between the age groups (table 1 and figure 3). It was the highest in the intermediate group and decreased significantly for the elderly group, from 19° to 16°.

The mean antero-posterior lever arm of the upper body CoM regarding L1 varied from 1 mm posteriorly for the young group, to 10 mm and 24 mm anteriorly for the intermediate and elderly groups respectively, with significant differences between each group (figure 4a), showing an anterior shift of the upper body CoM with age. The

standard deviation for the antero-posterior lever arm was high among all age groups and was the highest for the intermediate group (20 mm).

Using the mean and standard deviation values of the antero-posterior lever arm for the young group, a reference corridor was defined as values inside the following data range : [mean +/- 2*standard deviation]. It was observed that 23% of the intermediate and 48% of the elderly subjects had an abnormally high antero-posterior lever arm (above mean + 2*standard deviation). The lateral lever arm had a mean value of 2 mm to the left among all the subjects with a mean standard deviation of 7 mm. It was not significantly different between the age groups.

Strength evolution with subject-specific boundary conditions:
For the high, normal and low strength models, the computed strength with subject-specific boundary conditions was significantly lower in the elderly group than for the other age groups (figure 4b). For the normal strength model, the strength resulting from the variation of the lever arm among all the subjects ranged from 860 to 4066 N. It represented a variation of 373% between the highest and the lowest highest value. A decrease by 28% and 27% in vertebral strength was observed for the normal and the weak models between the young group and the elderly, from 2527 N to 1820 N and from 1622 N to 1183 N respectively. The loss was higher for the strong model (35%, from 3710 N to 2430 N). For all strength levels, the standard deviation was the highest in the intermediate group.

The load to strength ratio was the lowest for the strong model vertebra with loading conditions of the young group and the highest for the weak model vertebra considering the elderly group loading conditions (figure 4c). For all vertebral strength levels, it was significantly higher in the elderly group than in the young group. For the normal vertebra, while a decrease of 28% of vertebral strength between those groups was observed, the load to strength ratio increased by 67%. In addition, whereas the strength of the normal vertebra was 8% lower in the intermediate group compared to the young group, the load to strength ratio raised up to 30% in those same groups.

Discussion

Vertebral fragility fractures are an increasing concern. Understanding how they occur is a critical issue for public health. The current standard for osteoporosis diagnosis is aBDM assessment by DXA. However, its vertebral fracture prediction accuracy is limited and DXA cannot be used to analyze sagittal alignment. In order to enhance fracture prediction accuracy, other parameters have to be included in the diagnosis of osteoporosis. This study aimed to investigate the direct link between sagittal alignment and vertebral strength estimation based on radiological data using barycentremetry and finite element analysis.

Pelvic, spinal and sagittal alignment parameters of asymptomatic adults ranging from 20 to 83 years old were studied. A combination of an increase in the thoracic kyphosis as well as the cervical lordosis and a loss of lumbar lordosis was observed with aging, which is consistent with other studies [9, 10]. In addition, pelvic tilt was significantly higher in the elderly group than in the other two age groups. Pelvic retroversion and increase in cervical lordosis are compensatory mechanisms adopted to prevent the upper body from falling forward as the individuals grow older [10] and to maintain a horizontal gaze direction. Despite those mechanisms, a more forward posture was observed for each step of aging among the studied population. The OD-HA sagittal angle, the SVA and the spinal inclination [OD-S1] increased with age [7–10]. Head should remain above the pelvis in order to maintain equilibrium and lowest effort. Because of that, the OD-HA angle was proven to stay within a narrow range among a healthy population [10]. The main difference between the OD-HA sagittal angle and the spinal inclination [OD-S1] is the inclusion of the femoral heads, which results in the inclusion of the direct compensatory mechanism of the pelvis.

Using barycentremetry, a validated method used to accurately estimate the position of body CoM [23], the location of the upper body CoM above L1 was computed. In this asymptomatic population, the lateral lever arm was always very close to zero. Between the young group and the elderly group, a shift of the antero-posterior lever arm of the upper body CoM from a negative to a positive value was observed, revealing a change from a backward to a forward position as age increases. It confirms the postural changes observed through the clinical parameters. Although compensatory mechanisms allowed keeping the odontoid over the axis of the femoral head relatively well, they did not keep the CoM of the upper body strictly over the L1 vertebra. Among the intermediate group, the dispersion of the upper body CoM location was higher than in the other two age groups. The transition phase of aging could be inside this age group, which might explain those results.

We used a finite element model to study how variations in the lever arm of the upper body CoM affected vertebral strength, using three vertebral models with different intrinsic strength. Those vertebral models were chosen to represent the variety of vertebral strength for the whole age spectrum. To confirm this and compare our results to the literature, uniaxial loading was also simulated for these three vertebral models (data not shown). When compared to Bouxsein et al [36] who estimated vertebral strength for young and older subjects, the strength models chosen in the current study are consistent. The normal strength and strong models (4334 – 7013 N) of our study are close to the young population's strength (5366 – 6572 N) [36]. In addition, the weak and normal strength models (3256 – 4334 N) are similar to the older population's vertebral strength (3464 – 4966 N) [36]. In our study, for the same strength model, a variation of an average of 30% in the strength was observed resulting from the lever arm modifications related to the aging process only. We thus showed that apart from the intrinsic strength, an apparent strength including posture is altered by modifications with age and might be relevant to consider.

The load to strength ratio was computed to take into account morphological differences. In a standing position, when simulating a young individual (combining the normal and high strength level vertebrae and the loading conditions corresponding to the young group), the calculated ratio ranges from 0.07 to 0.1, which is consistent with the ratios observed [36] for a population with comparable age. When an alteration of the posture was included (elderly group), translated by a shift of the antero-posterior lever arm, the ratio could be up to 1.7 times higher. Our study offers a method to integrate those elements and refine vertebral strength estimation for critical populations.

This study presents some limitations. First, the geometry and mechanical properties were fixed. Promising results have been presented to estimate the material properties of the vertebra with biplanar radiography [13], and could be used in future studies. However, keeping unique models with identified strength levels was useful to highlight the effects of postural changes with age on vertebral strength independently of already observed changes in geometry or mechanical properties with age [37, 38]. In addition, muscle forces were not taken into account in the load estimation, only gravity loads were computed. In the standing position, for asymptomatic individuals, the subject is supposedly in an effortless position, which could indicate that the muscles forces are low. Also, the results obtained with this simplified model are consistent with the literature [36]. Finally, although the results were obtained on a fair sample size, it is a cross sectional-study, and a larger longitudinal set of data is needed to understand when the changes occur. An ulterior prospective study could be particularly interesting to assess the link between vertebral fracture occurrence and the current results.

In conclusion, we proposed a method to introduce in vivo loading into vertebral fracture risk assessment. The results confirmed that posture is different among older population and we were able to quantify and illustrate how those differences would affect vertebral strength. Further studies are needed to validate our observations, but those preliminary results indicate the importance of sagittal alignment when screening patients for osteoporosis. This study is a further step to reach a fully personalized finite element analysis for the evaluation of vertebral strength and fracture risk, including both personalized strength and personalized load.

Figures

Table 1 Results of the measurements of the spinal, pelvic and postural alignment parameters (*** = p<0.001, **=p<0.01, *=p<0.05), M mean, SD standard deviation, ns non-significant, Y young, I intermediate, E elderly

Fig 1 Sagittal alignment parameters, (a) SVA (mm) (post. Posterior, sup. Superior), (b) OD-HA sagittal angle (°), (c) Spinal inclination [OD-S1] (°)

Fig 2 (a) Example of the reconstructed body envelope used to compute the upper body CoM above L1, segments in yellow are included in the computation (arms were place along the body for the CoM computation), the CoM and its vertical line are located on the envelope, as well as the subject's L1 vertebra, (b) example of the personalized loading conditions of the normal strength level vertebral model and the CoM location

Fig 3 Average sagittal L1 orientation and antero-posterior lever arm of the upper body CoM above L1 against the normal strength vertebral model

Fig 4 (a) Antero-posterior distance (mean and 1*SD) between the upper body CoM above L1 and the center of L1, (b) computed strength (mean and 1*SD) and (c) load to strength ratio (mean and 1*SD) resulting from the personalization of boundary conditions specific to the upper body CoM of the three FEM of L1 vertebra with identified strength level: weak (1900 N), normal (3200 N), and strong (5000 N) for 117 subjects divided in three age groups. Results of statistical tests to assess differences between the groups (*** = p<0.001, *=p<0.05)
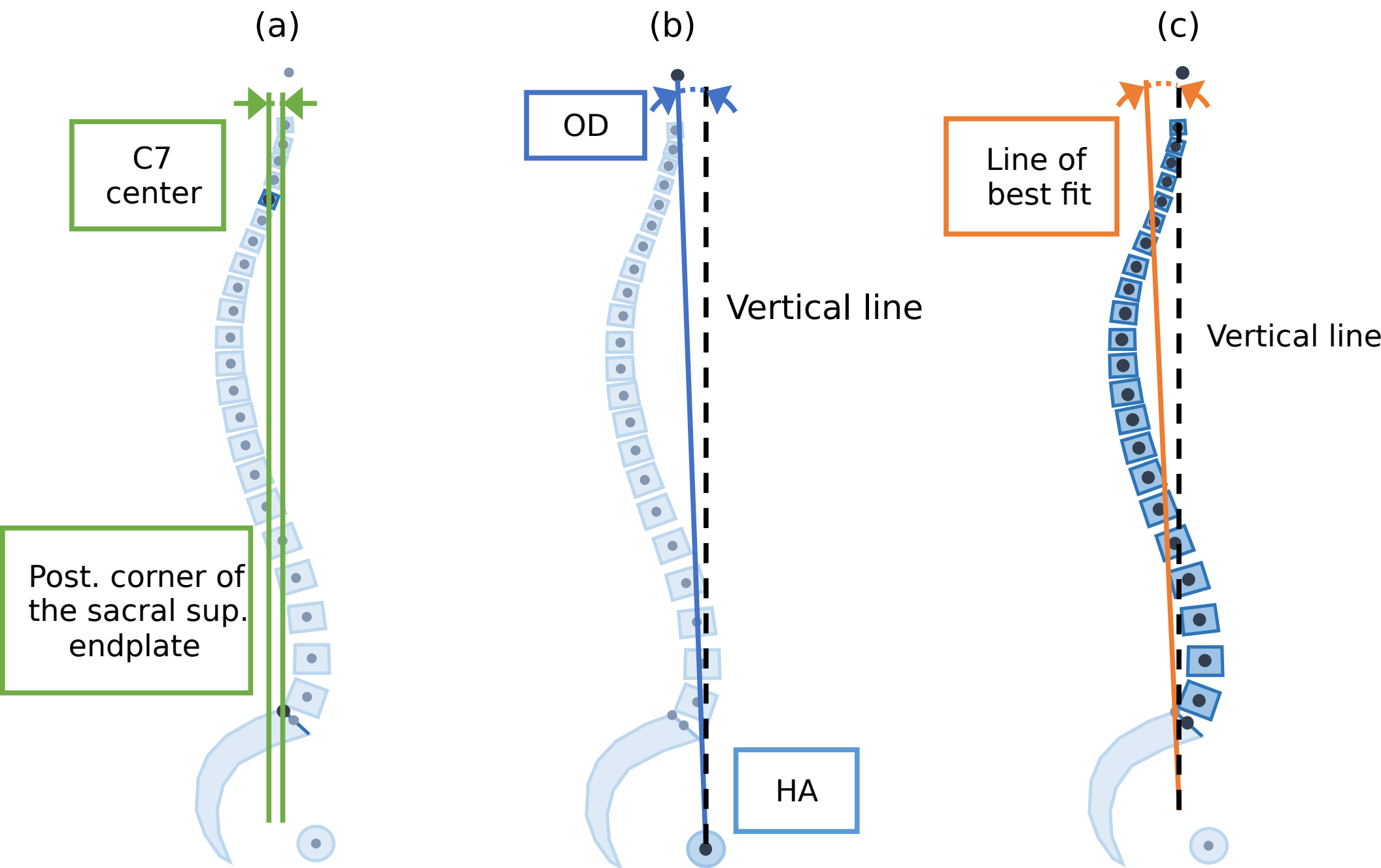
References

1. Johnell O, Kanis JA (2006) An estimate of the worldwide prevalence and disability associated with osteoporotic fractures. Osteoporos Int 17:1726–1733. https://doi.org/10.1007/s00198-006-0172-4

2. Bliuc D, Nguyen ND, Milch VE, et al (2009) Mortality risk associated with low-trauma osteoporotic fracture and subsequent fracture in men and women. JAMA 301:513–521. https://doi.org/10.1001/jama.2009.50

3. Löffler MT, Jacob A, Valentinitsch A, et al (2019) Improved prediction of incident vertebral fractures using opportunistic QCT compared to DXA. Eur Radiol 29:4980–4989. https://doi.org/10.1007/s00330-019-06018-w

4. Cosman F, Krege JH, Looker AC, et al (2017) Spine fracture prevalence in a nationally representative sample of US women and men aged ≥40 years: results from the National Health and Nutrition Examination Survey (NHANES) 2013-2014. Osteoporos Int J Establ Result Coop Eur Found Osteoporos Natl Osteoporos Found USA 28:1857–1866. https://doi.org/10.1007/s00198-017-3948-9

5. Oudshoorn C, Hartholt K, Zillikens C, et al (2012) Emergency department visits due to vertebral fractures in the Netherlands, 1986-2008: Steep increase in the oldest old, strong association with falls. Inj Int J Care Inj 43:458–461. https://doi.org/10.1016/j.injury.2011.09.014

6. Wang H, Li C, Xiang Q, et al (2012) Epidemiology of spinal fractures among the elderly in Chongqing, China. Injury 43:2109–2116. https://doi.org/10.1016/j.injury.2012.04.008

7. Hu Z, Man GCW, Kwok AKL, et al (2018) Global sagittal alignment in elderly patients with osteoporosis and its relationship with severity of vertebral fracture and quality of life. Arch Osteoporos 13:95. https://doi.org/10.1007/s11657-018-0512-y

8. Fechtenbaum J, Etcheto A, Kolta S, et al (2016) Sagittal balance of the spine in patients with osteoporotic vertebral fractures. Osteoporos Int J Establ Result Coop Eur Found Osteoporos Natl Osteoporos Found USA 27:559–567. https://doi.org/10.1007/s00198-015-3283-y

9. Bassani T, Galbusera F, Luca A, et al (2019) Physiological variations in the sagittal spine alignment in an asymptomatic elderly population. Spine J 19:1840–1849. https://doi.org/10.1016/j.spinee.2019.07.016

10. Amabile C, Le Huec J-C, Skalli W (2018) Invariance of head-pelvis alignment and compensatory mechanisms for asymptomatic adults older than 49 years. Eur Spine J 27:458–466. https://doi.org/10.1007/s00586-016-4830-8

11. Crawford RP, Cann CE, Keaveny TM (2003) Finite element models predict in vitro vertebral body compressive strength better than quantitative computed tomography. Bone 33:744–750. https://doi.org/10.1016/S8756-3282(03)00210-2

12. LI D, XIAO Z, WANG G, ZHAO G (2014) Novel, fast and efficient image-based 3D modeling method and its application in fracture risk evaluation. Exp Ther Med 7:1583–1590. https://doi.org/10.3892/etm.2014.1645

13. Choisne J, Valiadis J-M, Travert C, et al (2018) Vertebral strength prediction from Bi-Planar dual energy x-ray absorptiometry under anterior compressive force using a finite element model: An in vitro study. J Mech Behav Biomed Mater 87:190–196. https://doi.org/10.1016/j.jmbbm.2018.07.026

14. Imai K (2011) Vertebral fracture risk and alendronate effects on osteoporosis assessed by a computed tomography-based nonlinear finite element method. J Bone Miner Metab 29:645–651. https://doi.org/10.1007/s00774-011-0281-9

15. Allaire BT, Lu D, Johannesdottir F, et al (2019) Prediction of incident vertebral fracture using CT-based finite element analysis. Osteoporos Int 30:323–331. https://doi.org/10.1007/s00198-018-4716-1
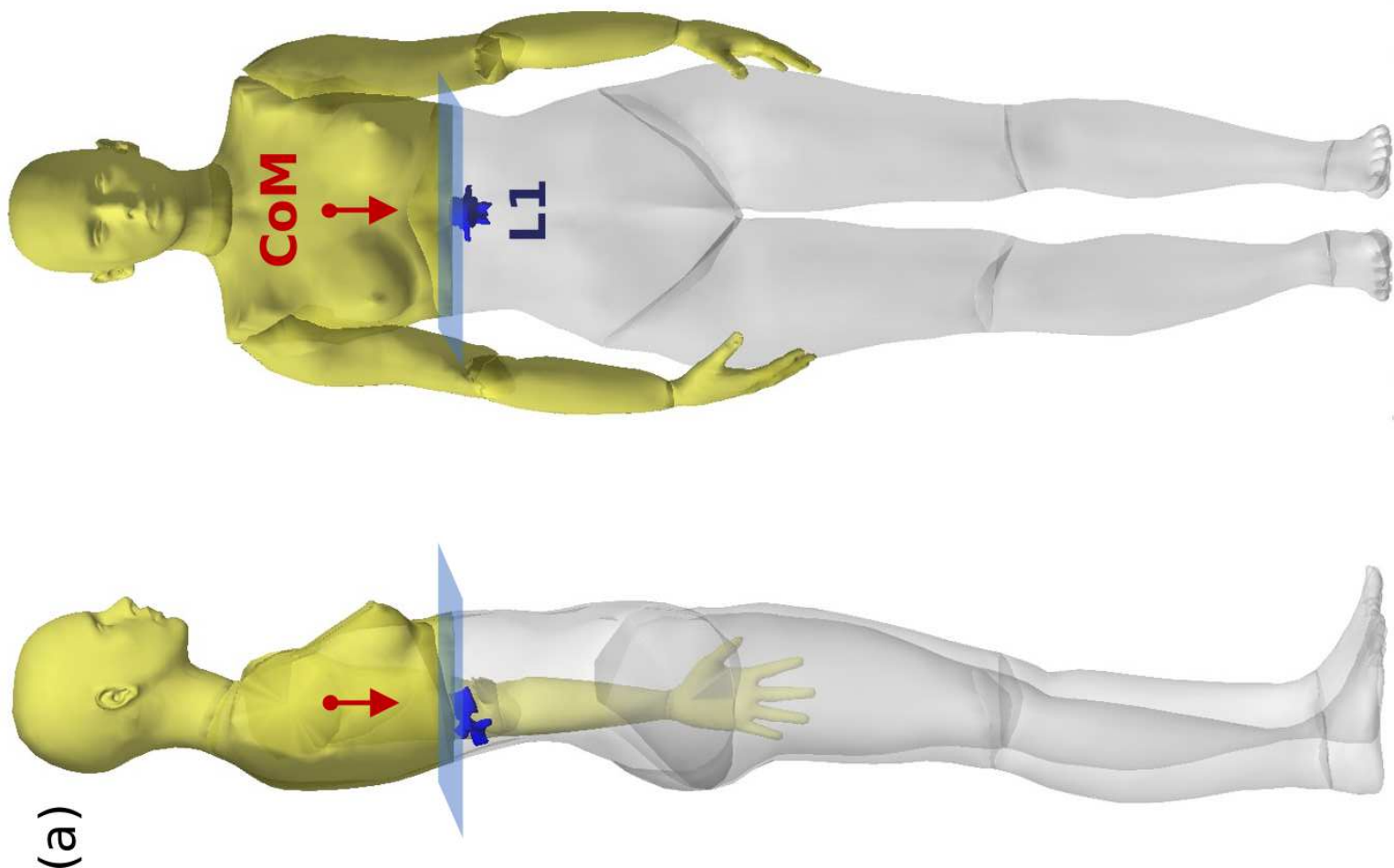
16. Briggs AM, van Dieën JH, Wrigley TV, et al (2007) Thoracic Kyphosis Affects Spinal Loads and Trunk Muscle Force. Phys Ther 87:595–607. https://doi.org/10.2522/ptj.20060119

17. Bruno AG, Anderson DE, D'Agostino J, Bouxsein ML (2012) The effect of thoracic kyphosis and sagittal plane alignment on vertebral compressive loading. J Bone Miner Res Off J Am Soc Bone Miner Res 27:2144–2151. https://doi.org/10.1002/jbmr.1658

18. Buckley JM, Kuo CC, Cheng LC, et al (2009) Relative strength of thoracic vertebrae in axial compression versus flexion. Spine J Off J North Am Spine Soc 9:478–485. https://doi.org/10.1016/j.spinee.2009.02.010

19. Travert C, Jolivet E, Sapin-de Brosses E, et al (2011) Sensitivity of patient-specific vertebral finite element model from low dose imaging to material properties and loading conditions. Med Biol Eng Comput 49:1355–1361. https://doi.org/10.1007/s11517-011-0825-0

20. COSSON P, DUVAL-BEAUPERE G (1993) Détermination personnalisée in vivo chez l'homme des efforts exercés sur les étages vertébraux thoraciques et lombaires en position debout et assise. Déterm Personnal Vivo Chez Homme Efforts Exerc Sur Étages Vertébraux Thorac Lombaires En Position Debout Assise 5:5–12

21. Mitton D, Deschênes S, Laporte S, et al (2006) 3D reconstruction of the pelvis from bi-planar radiography. Comput Methods Biomech Biomed Engin 9:1–5. https://doi.org/10.1080/10255840500521786

22. Humbert L, De Guise JA, Aubert B, et al (2009) 3D reconstruction of the spine from biplanar X-rays using parametric models based on transversal and longitudinal inferences. Med Eng Phys 31:681–687. https://doi.org/10.1016/j.medengphy.2009.01.003

23. Nérot A, Choisne J, Amabile C, et al (2015) A 3D reconstruction method of the body envelope from biplanar X-rays: Evaluation of its accuracy and reliability. J Biomech 48:4322–4326. https://doi.org/10.1016/j.jbiomech.2015.10.044

24. Thenard T, Vergari C, Hernandez T, et al (2019) Analysis of Center of Mass and Gravity-Induced Vertebral Axial Torque on the Scoliotic Spine by Barycentremetry. Spine Deform 7:525–532. https://doi.org/10.1016/j.jspd.2018.11.007

25. Dubousset J, Charpak G, Skalli W, et al (2010) Eos: a new imaging system with low dose radiation in standing position for spine and bone & joint disorders. J Musculoskelet Res 13:1–12. https://doi.org/10.1142/S0218957710002430

26. Faro FD, Marks MC, Pawelek J, Newton PO (2004) Evaluation of a functional position for lateral radiograph acquisition in adolescent idiopathic scoliosis. Spine 29:2284–2289. https://doi.org/10.1097/01.brs.0000142224.46796.a7

27. Gajny L, Ebrahimi S, Vergari C, et al (2019) Quasi-automatic 3D reconstruction of the full spine from low-dose biplanar X-rays based on statistical inferences and image analysis. Eur Spine J 28:658–664. https://doi.org/10.1007/s00586-018-5807-6

28. Legaye J, Duval-Beaupère G, Hecquet J, Marty C (1998) Pelvic incidence: a fundamental pelvic parameter for three-dimensional regulation of spinal sagittal curves. Eur Spine J 7:99–103. https://doi.org/10.1007/s005860050038

29. Jackson RP, McManus AC (1994) Radiographic Analysis of Sagittal Plane Alignment and Balance in Standing Volunteers and Patients with Low Back Pain Matched for Age, Sex, and Size: A Prospective Controlled Clinical Study. Spine 19:1611–1618

30. Amabile C, Pillet H, Lafage V, et al (2016) A new quasi-invariant parameter characterizing the postural alignment of young asymptomatic adults. Eur Spine J 25:3666–3674. https://doi.org/10.1007/s00586-016-4552-y

31. Lafage V, Schwab F, Patel A, et al (2009) Pelvic Tilt and Truncal Inclination: Two Key Radiographic Parameters in the Setting of Adults With Spinal Deformity. Spine 34:E599. https://doi.org/10.1097/BRS.0b013e3181aad219

32. Amabile C, Choisne J, Nérot A, et al (2016) Determination of a new uniform thorax density representative of the living population from 3D external body shape modeling. J Biomech 49:1162–1169. https://doi.org/10.1016/j.jbiomech.2016.03.006

33. Grados F, Marcelli C, Dargent-Molina P, et al (2004) Prevalence of vertebral fractures in French women older than 75 years from the EPIDOS study. Bone 34:362–367. https://doi.org/10.1016/j.bone.2003.11.008

34. Melton LJ, Lane AW, Cooper C, et al (1993) Prevalence and incidence of vertebral deformities. Osteoporos Int 3:113–119. https://doi.org/10.1007/BF01623271

35. Pennec GL, Campana S, Jolivet E, et al (2014) CT-based semi-automatic quantification of vertebral fracture restoration. Comput Methods Biomech Biomed Engin 17:1086–1095. https://doi.org/10.1080/10255842.2012.736968

36. Bouxsein ML, Melton LJ, Riggs BL, et al (2006) Age- and Sex-Specific Differences in the Factor of Risk for Vertebral Fracture: A Population-Based Study Using QCT. J Bone Miner Res 21:1475–1482. https://doi.org/10.1359/jbmr.060606

37. Kolta S, Kerkeni S, Travert C, et al (2012) Variations in vertebral body dimensions in women measured by 3D-XA: a longitudinal in vivo study. Bone 50:777–783. https://doi.org/10.1016/j.bone.2011.12.005

38. Riggs BL, Melton Iii LJ, Robb RA, et al (2004) Population-based study of age and sex differences in bone volumetric density, size, geometry, and structure at different skeletal sites. J Bone Miner Res Off J Am Soc Bone Miner Res 19:1945–1954. https://doi.org/10.1359/JBMR.040916

Table1　　　　　　　　　　　　　　　　　　　Click here to access/download;Table;Table1.eps ⬇

Parameters	Young (N= 62) M (1*SD)	Intermediate (N = 26) M (1*SD)	Elderly (N= 29) M (1*SD)	p-value Y vs I	Y vs E	I vs E
Age (years)	27 (5)	49 (7)	70 (5)	-	-	-
BMI	23 (3)	24 (3)	26 (3)	0.11	**	0.06
Spinal parameters						
C3C7 curvature (°)	4.7 (10.3)	-2.9 (8.2)	-4.5 (12.4)	***	**	0.57
T4-T12 thoracic kyphosis (°)	34.9 (11.4)	39.4 (9.5)	40.4 (10.8)	0.06	*	0.71
L1-S1 lumbar lordosis (°)	57.9 (11.8)	54.6 (9)	50.3 (12.4)	0.16	**	0.14
L1 sagittal orientation (°)	-18.3 (5.4)	-19.3 (5.2)	-15.7 (6.1)	0.45	0.06	*
Pelvic parameters						
PI (°)	50.1 (10.9)	53.1 (8.9)	53.8 (12.4)	0.19	0.18	0.8
SS (°)	41.1 (8.7)	37.3 (6.9)	36.1 (9.3)	0.07	*	0.57
PT (°)	9.1 (6.3)	15.8 (4.6)	17.8 (7.9)	***	***	0.26
Global sagittalalignment						
OD-HA sagittal angle (°)	-2.0 (1.9)	-1.7 (2.4)	0.4 (2.8)	0.49	***	**
SVA (cm)	-1.5(2.2)	0.2(2.6)	2.2(2.6)	**	***	**
Spinal inclination [OD-S1] (°)	-2.9 (2.6)	-0.9 (3.5)	1.9 (3.5)	*	***	**

Fig1

(a)

C7 center

Post. corner of the sacral sup. endplate

(b)

OD

Vertical line

HA

(c)

Line of best fit

Vertical line

Fig2

Click here to access/download;Figure;Fig2.eps ±

(a)

(b)

CoM

L1

CoM

Fig3

Anteroposterior lever arm — CoM vertical line — -18° — Young

Anteroposterior lever arm — CoM vertical line — -19° — Intermediate

Anteroposterior lever arm — CoM vertical line — -16° — Elderly

Fig4

Click here to access/download;Figure;Fig4.eps ⬇